

# Urban Visibility Hotspots: Quantifying Building Vertex Visibility from Connected Vehicle Trajectories using Spatial Indexing

1<sup>st</sup> Artur Grigorev

Faculty of Engineering and IT  
University of Technology Sydney  
Sydney, Australia  
ORCID: 0000-0001-6875-3568

2<sup>nd</sup> Adriana-Simona Mihăiță

Faculty of Engineering and IT  
University of Technology Sydney  
Sydney, Australia  
ORCID: 0000-0001-7670-5777

**Abstract**—Effective placement of Out-of-Home advertising and street furniture requires accurate identification of locations offering maximum visual exposure to target audiences, particularly vehicular traffic. Traditional site selection methods often rely on static traffic counts or subjective assessments. This research introduces a data-driven methodology to objectively quantify location visibility by analyzing large-scale connected vehicle trajectory data (sourced from Compass IoT) within urban environments. We model the dynamic driver field-of-view using a forward-projected visibility area for each vehicle position derived from interpolated trajectories. By integrating this with building vertex locations extracted from OpenStreetMap, we quantify the cumulative visual exposure, or “visibility count”, for thousands of potential points of interest near roadways. The analysis reveals that visibility is highly concentrated, identifying specific “visual hotspots” that receive disproportionately high exposure compared to average locations. The core technical contribution involves the construction of a BallTree spatial index over building vertices. This enables highly efficient ( $O(\log N)$  complexity) radius queries to determine which vertices fall within the viewing circles of millions of trajectory points across numerous trips, significantly outperforming brute-force geometric checks. Analysis reveals two key findings: 1) Visibility is highly concentrated, identifying distinct ‘visual hotspots’ receiving disproportionately high exposure compared to average locations. 2) The aggregated visibility counts across vertices conform to a Log-Normal distribution.

**Index Terms**—Connected Vehicle Trajectories, Visibility Hotspots, Visibility Analysis, Spatial Indexing, Urban Analytics

## I. INTRODUCTION

Out-of-Home (OOH) advertising remains a vital channel in the marketing mix, with significant investment directed towards formats like billboards and street furniture, particularly in urban centres [1]. The advent of digital OOH (DOOH) offers enhanced flexibility, yet the fundamental challenge of effective media planning persists. Traditional methods for selecting OOH locations often rely on static demographic data or aggregated traffic volumes, which may inadequately capture the dynamic reality of urban mobility and actual audience visibility [2]. Simple Opportunity To See (OTS) metrics often overestimate true exposure, failing to account for viewing angles, vehicle dynamics (e.g. duration of stops), obstructions, and travel paths [1].

To address these limitations, data-driven approaches that take advantage of real-world movement data are gaining traction. Connected vehicle technologies generate vast amounts of granular trajectory data, offering a detailed view of how vehicles navigate the urban landscape. Concurrently, open geospatial datasets provide information about the geometry of built environment. This research focuses on utilizing these data sources to develop a more precise understanding of visibility, specifically targeting the exposure of urban building features from the perspective of vehicular traffic.

This paper introduces a methodology to quantify the visibility of urban building vertices using connected vehicle trajectory data (sourced from the Compass IoT platform, an Australian startup collecting trajectory and telemetry data from connected vehicles across Australia, New Zealand, UK and USA) and building footprint data (from OpenStreetMap). We address the computational challenge of analysing large-scale trajectory data against complex urban geometry by employing efficient spatial indexing techniques, specifically BallTree structures. Our approach involves: (1) processing and interpolating connected vehicle trajectories to regular time intervals and calculating instantaneous vehicle bearing; (2) defining a dynamic, forward-looking viewing area for each vehicle position; (3) extracting vertices from OpenStreetMap building polygons; (4) utilizing a BallTree index for efficient querying of building vertices within the vehicles’ viewing areas; and (5) aggregating visibility counts per building vertex across numerous trajectories.

The primary contribution of this work is a scalable framework for generating granular, objective metrics of building vertex visibility based on observed traffic patterns. This provides a quantitative basis for identifying high-exposure locations (“visual hotspots”) relevant for applications such as optimizing the placement of OOH advertising assets like billboards or digital screens, informing urban design, or enhancing navigation systems.

## II. RELATED WORKS

The challenge of optimizing Out-of-Home (OOH) advertising placement and measuring its effectiveness has spurred research into data-driven methodologies that move beyond traditional static analyses [1]. Traditional methods, often relying on aggregated traffic counts or area demographics [2], usually do not capture the dynamic nature of driver mobility and the nuances of actual advertisement visibility [1]. This review situates our work within the context of two primary data-driven approaches identified in the literature: traffic simulation and real-world trajectory data analysis.

Traffic simulation including macroscopic, microscopic, and agent-based models (ABM), is a well-established tool in transportation research for analyzing network performance, safety, and demand [3]–[5]. While microscopic and ABM simulations offer the potential to model individual viewer (pedestrian or vehicle) paths and incorporate environmental factors affecting visibility [3], [6], their documented application specifically for quantifying geometric OOH visibility or optimizing placement based on such metrics appears limited. Approaches like Cellular Automata (CA) have been used to model the reach of mobile transit advertising, focusing on information spread rather than precise geometric visibility [7].

Our research aligns more closely with approaches utilizing real-world trajectory data. This data, sourced from GPS devices, mobile phones, or public transport smart cards, captures observed movement patterns [8]. Analysis techniques applied to such data include preprocessing [9], clustering common routes [10], predicting destinations [11], and inferring trip purpose [12], often with the goal of enabling targeted advertising. For instance, research using South East Queensland’s smart card data demonstrated optimizing ad placement in transit networks based on inferred passenger activities [12]. Similarly, destination prediction algorithms, developed partly by Australian researchers using taxi GPS data, aim to inform relevant advertising along predicted routes [11]. The work by Fong et al. (2013) [13] explores optimal spatial groups in sensor networks to maximize coverage or effect using clustering and optimization techniques. The obtained visibility data in our research could potentially inform optimal roadside sensor placements, identifying locations frequently observed by vehicular traffic.

A particularly relevant example is the SmartAdP visual analytics system [14]. SmartAdP uses large-scale historical taxi trajectory data to help planners select optimal billboard locations. It derives metrics like traffic volume, speed, reach (coverage), and Opportunities-To-See (OTS) directly from the trajectory data and relies on spatial indexing for efficient querying [14]. While highly relevant in its use of trajectory data and focus on placement optimization, SmartAdP differs from our approach in key ways: it relies on historical taxi data (which may not represent all traffic), uses derived metrics as proxies for exposure rather than direct geometric visibility calculation, and focuses on billboard locations rather than granular building vertex visibility.

Furthermore, the concept of visibility itself is complex. Industry standards like Australia’s MOVE system attempt to quantify it by adjusting OTS based on factors like viewing angle, speed, distance, and ad characteristics, using data from travel surveys and eye-tracking rather than dynamic simulation or granular trajectory-based geometric checks [1], [15]. Other research domains utilize Geographic Information Systems (GIS) with line-of-sight (LoS) or viewshed analyses [16], [17], typically for static viewpoints or environmental assessment, highlighting the geometric tools potentially adaptable for dynamic analysis.

Our work contributes to this landscape by: 1) Utilizing high-frequency (up to every 5 second trajectory updates) connected vehicle location and direction data which may offer broader coverage of traffic (includes passenger vehicles, buses, than specific sources like taxis or smart cards. 2) Focusing specifically on quantifying the geometric visibility of discrete urban features (building vertices from OSM) rather than relying solely on proximity or traffic volume metrics. 3) We also use BallTree spatial indexing explicitly for the efficient execution of numerous dynamic point-in-circle visibility queries derived from vehicle trajectories, enabling scalability. By combining these elements, we aim to provide a granular and computationally efficient method for assessing urban visibility potential from the perspective of real moving vehicles.

1) *Study Area*: The geographical focus of this research is the inner-city suburb of **Waterloo** and its immediate surroundings, located approximately 3-4 kilometers south of the Sydney Central Business District (CBD) in New South Wales, Australia. Waterloo is characterized by a dense urban landscape, featuring a mix of historical residential terraces, contemporary high-density apartment complexes, commercial buildings, cafes and public parks.

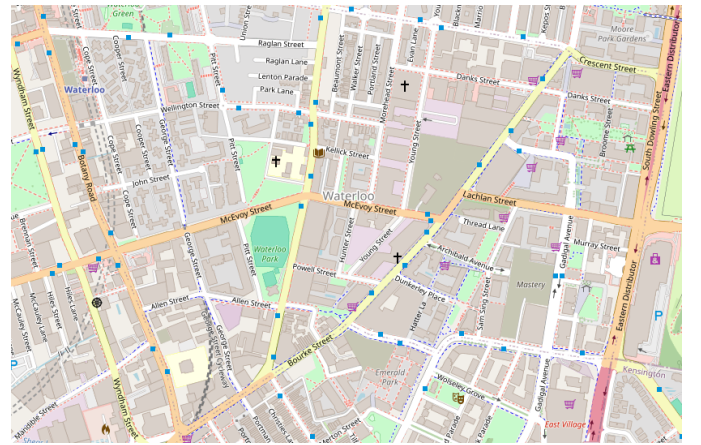


Fig. 1. Map of the Waterloo study area. (Image source: OpenStreetMap)

The specific region subjected to data analysis in this study is defined by the following geographical bounding box, using the **WGS84 coordinate system (EPSG:4326)**:

This bounding box encapsulates the core of Waterloo and includes portions of adjacent suburbs such as Redfern, Zetland,

TABLE I  
GEOGRAPHICAL BOUNDING BOX (WGS84 COORDINATE SYSTEM -  
EPSG:4326)

Coordinate Type	Minimum Value	Maximum Value
Longitude	151.18943° E	151.21681° E
Latitude	-33.91441° S	-33.89325° S

and Alexandria. This selection provides a representative sample of inner-Sydney urban morphology, featuring a variety of road network types (major arterials, local streets) and mix of building densities, suitable for analyzing vehicular visibility patterns in a complex built environment. Building footprint data from OpenStreetMap and connected vehicle trajectory data from Compass IoT (limited to 2000 trips over 1 week of observations from the 1-7 march, year 2024) were filtered and analyzed specifically within this defined area.

### III. METHODOLOGY

The foundation for this analysis comprises two key processed datasets derived from raw sources. Firstly, we utilize a set of pre-processed connected vehicle trajectories, sourced from Compass IoT, which have been interpolated to provide a consistent vehicle position (latitude, longitude) and calculated bearing every 5 seconds within the Waterloo study area. Secondly, building footprint data obtained from OpenStreetMap. Instead of relying solely on the original vertices defining the building polygons, we interpolate additional points along each polygon edge segment. This ensures that the representation of the building outline consists of points spaced no more than 10 meters apart. This densified set of building points serves as the target features for our visibility assessment. The core objective of the subsequent methodology is to determine how frequently these densified building points fall within the dynamic viewing area projected forward from the moving vehicles.

#### A. Spatial Querying and Visibility Calculation

Addressing the computational intensity of determining which densified building points fall inside numerous viewing circles requires an efficient spatial querying strategy.

**BallTree Spatial Indexing:** The core technique used is spatial indexing using a BallTree structure. This approach avoids brute-force distance calculations for every building point-circle pair, offering significant performance gains. The construction process involves several key steps: 1) Latitude/longitude coordinates of the densified building edge points (generated as described previously) are converted to radians, suitable for spherical calculations. 2) The BallTree index is constructed using these radian coordinates, specifically utilizing the “haversine” metric to ensure accurate great-circle distance computations. 3) A mapping is maintained to link the internal index of each point within the BallTree structure back to its unique identifier (representing its position along a specific building edge). The BallTree hierarchically partitions the building point data into nested hyperspheres (balls), enabling rapid pruning of the search space during distance-based queries.

**Point-in-Circle Queries:** With the BallTree index in place, the visibility calculation proceeds for each interpolated trajectory point possessing a valid bearing. The querying process follows these steps: 1) The viewing circle center is calculated (50m ahead along the bearing) using the `CalculateDestinationPoint` function. 2) The physical radius (50 meters) is converted into an equivalent angular radius ( $R_{angular}$ ) based on the Earth’s radius, appropriate for the Haversine distance metric used by the BallTree. 3) The BallTree’s `query_radius` method is invoked, supplying the circle center coordinates (in radians) and the calculated angular radius. This efficiently retrieves the indices of all densified building points located within the specified 50-meter great-circle distance from the viewing circle’s center. 4) For each building point index returned by the query, a corresponding counter (representing the visibility count for that specific point during the trip) is incremented. This procedure is repeated for every valid point across all trajectories processed.

The detailed procedure for calculating these visibility counts for a single trip, operating on the densified building points, is formalized in Algorithm 1.

#### B. Aggregation and Analysis

Following the per-trip visibility calculations which yield counts for densified building points, the results are consolidated to provide an overall measure of visibility for each point across the entire dataset.

**Visibility Count Aggregation:** The primary goal here is to aggregate the visibility counts obtained for each densified building point during individual trips into a single total count. The aggregation logic proceeds as follows: 1) Per-trip visibility results (mapping point identifiers to counts) are processed, grouping counts by unique densified building point. A key derived from rounded coordinates is typically used to ensure these points are uniquely identified across different processing batches or potential floating-point discrepancies. 2) For each unique building point key, the visibility counts accumulated across all trips are summed to yield a final `total_count`. 3) The aggregated results are stored, typically in a structure mapping the unique point key back to its original coordinates and the calculated `total_count`. This aggregated count represents the overall frequency with which each densified building point along building outlines was found within a vehicle’s viewing area across the studied trajectories.

#### C. Trajectory and Visibility Visualization

Figure 2 illustrates the output of the trajectory processing and the definition of viewing areas used in the visibility modeling for a single vehicle trip (48 interpolated points) within the study area. The blue line represents the vehicle’s path derived from the 5-second interpolation, while the red circles depict the 100-meter diameter viewing areas projected 50 meters ahead along the vehicle’s bearing at each point. These circles define the regions within which the \*densified building points\* were queried for visibility using the BallTree

---

**Algorithm 1** Visibility Calculation for a Single Trip using BallTree (Densified Building Points)

---

**Require:** Trip data  $T$  (list of points with lat, lon, bearing)**Require:** Densified building point spatial index  $B_{tree}$  (BallTree)**Require:** Mapping  $M_{id}$  from tree index to original point identifier  $p_{id}$ **Require:** Circle radius  $R_{meters}$ **Ensure:** Map  $V_{trip}$  of {point\_id: visibility\_count} for trip  $T$ 

```
1:  $N_{points} \leftarrow \text{GETNUMBEROFPPOINTS}(B_{tree})$  ▷ Total number of densified points
2: Initialize integer array  $C_{point\_counts}$  of size  $N_{points}$  with zeros
3:  $R_{angular} \leftarrow R_{meters} / \text{EARTH\_RADIUS\_METERS}$  ▷ Convert radius to radians
4: for each point  $p$  in  $T$  do
5:   if  $p.bearing$  is valid then
6:      $(lat_c, lon_c) \leftarrow \text{CALCULATEDESTINATIONPOINT}(p.lat, p.lon, p.bearing, R_{meters})$  ▷ Calculate circle center
7:     if  $lat_c$  is valid and  $lon_c$  is valid then
8:        $coord\_c^{rad} \leftarrow \text{TORADIANS}([lat_c, lon_c])$  ▷ Convert center to radians
9:        $indices \leftarrow \text{QUERYBALLTREERADIUS}(B_{tree}, coord\_c^{rad}, R_{angular})$  ▷ Find points in circle
10:      for each index  $idx$  in  $indices[0]$  do ▷ Query returns list of lists
11:         $C_{point\_counts}[idx] \leftarrow C_{point\_counts}[idx] + 1$ 
12:      end for
13:    end if
14:  end if
15: end for
16: Initialize empty map  $V_{trip}$ 
17: for  $i \leftarrow 0$  to  $N_{points} - 1$  do
18:   if  $C_{point\_counts}[i] > 0$  then
19:      $p_{id} \leftarrow M_{id}[i]$  ▷ Get original point ID from map
20:      $V_{trip}\{p_{id}\} \leftarrow C_{point\_counts}[i]$  ▷ Store count in result map
21:   end if
22: end for
23: return  $V_{trip}$ 
```

---

index. This visualization helps understand the spatial coverage of the visibility assessment along an individual route.

#### D. Aggregated Visibility Distribution

The aggregated visibility counts across all processed trajectories exhibit a highly skewed distribution, as shown in Figure 3. This histogram plots the total number of times each unique building vertex was captured within a viewing circle. The x-axis represents the aggregated visibility count, while the y-axis shows the number of vertices falling into each count bin, presented on a logarithmic scale to accommodate the wide range of values. The distribution clearly indicates that a vast majority of building vertices have very low visibility counts, while a small number of vertices achieve significantly higher counts, forming a long tail characteristic of phenomena where exposure is concentrated. This skewness suggests that overall visibility is dominated by relatively few locations within the study area.

To further explore the spatial concentration of visibility, Figure 4 visualizes the locations of building vertices color-coded according to their aggregated visibility quantile group. This plot distinctly highlights the vertices falling within the highest visibility percentiles (e.g., top 1%, 95th-99th percentile) compared to the vast majority of low-visibility points (e.g., bottom 90%). The visualization confirms the spatial

clustering of high-visibility vertices, often located at prominent intersections or along major thoroughfares within the Waterloo area. Furthermore, the plot quantifies the contribution of these top quantile groups to the overall visibility sum, typically demonstrating a Pareto-like principle where a small fraction of vertices accounts for a large percentage of the total visibility events captured across all trajectories (e.g. top 10% of points gains around 39.5% of total visibility).

#### E. Statistical Distribution of Visibility

The aggregated visibility counts for the 34,495 unique building vertices with non-zero visibility were fitted to several common probability distributions. The goal was to characterize the overall distribution of visibility across the study area. Table II summarizes the estimated parameters for each fitted distribution, along with goodness-of-fit statistics including the Kolmogorov-Smirnov (K-S) statistic (D) and the 1-Wasserstein distance. Lower values for D and Wasserstein distance generally indicate a better fit to the empirical data.

Based on the goodness-of-fit statistics, particularly the K-S statistic and the Wasserstein distance, the Log-Normal distribution provides the best fit to the empirical visibility data among the tested distributions, followed by the Inverse Gamma and Exponential distributions. This confirms the highly skewed, long-tailed nature of vertex visibility observed

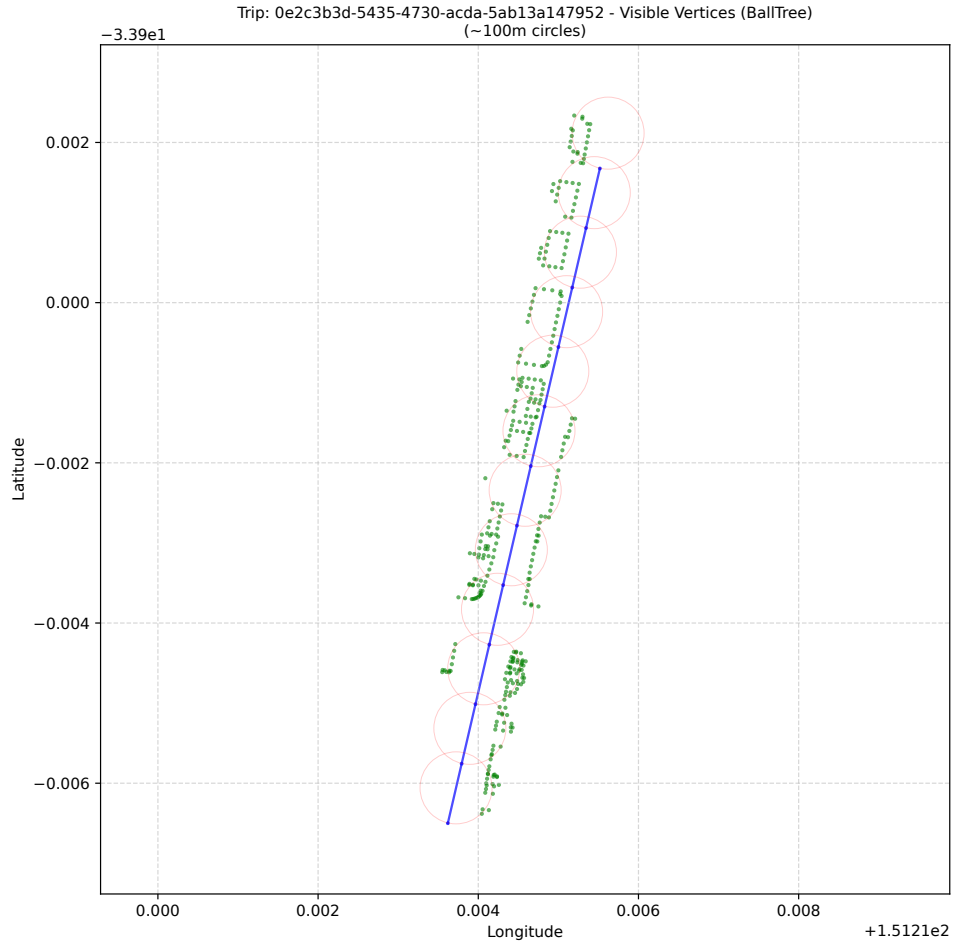


Fig. 2. Example interpolated trajectory trace and associated viewing circles for a single trip (ID ending 2174) within the Waterloo study area. Blue line indicates vehicle path (48 points), red circles represent the 100m diameter forward viewing areas used for visibility analysis.

TABLE II  
DISTRIBUTION FITTING RESULTS FOR AGGREGATED VERTEX VISIBILITY COUNTS (N=34,495). PARAMETERS SHOWN ARE SHAPE (S, A, C), LOCATION (LOC), AND SCALE. K-S P-VALUES WERE EFFECTIVELY ZERO ( $< 10^{-70}$ ) FOR ALL FITS SHOWN.

Distribution	K-S Stat (D)	Wasserstein Dist.	loc	scale	a	c	s
Log-Normal	0.0489	40.4802	-23.5784	263.5925	—	—	1.0332
Gamma	0.9936	413.0533	1.0000	2.6506	0.0029	—	—
Exponential	0.0493	62.1045	1.0000	413.0612	—	—	—
Weibull (min)	0.1324	71.2408	1.0000	299.4076	—	0.7558	—
Normal	0.2358	259.2370	414.0612	573.7056	—	—	—
Inverse Gamma	0.0482	55.1729	-108.3701	670.4057	2.2225	—	—
Gumbel (R)	0.0858	96.7158	234.0655	259.4164	—	—	—

TABLE III

\*

K-S: Kolmogorov-Smirnov statistic. Wasserstein Dist.: 1-Wasserstein distance. Lower values indicate better fit. Parameters a, c, s are shape parameters specific to certain distributions. '—' indicates parameter not applicable for the distribution.

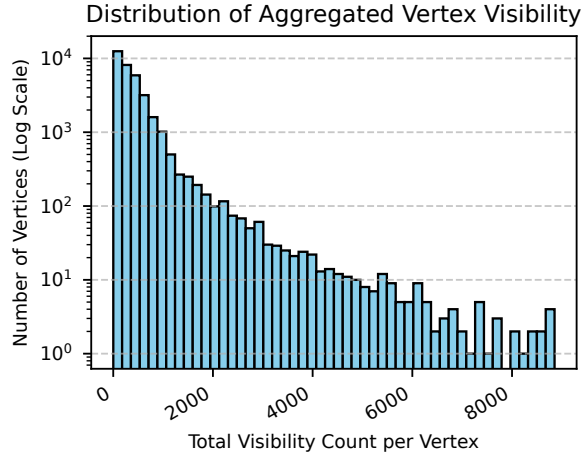


Fig. 3. Frequency distribution of aggregated visibility counts per building vertex across all processed trajectories. The y-axis (Number of Vertices) is plotted on a logarithmic scale.

in the histogram (Figure 3). The poor fit of the Normal distribution further emphasizes this non-Gaussian characteristic.

#### IV. DISCUSSION

The findings of this research provide an overview of the nature of urban visibility from a perspective of vehicular trajectories. The primary observation that building vertex visibility is highly concentrated in specific “visual hotspots” has direct implications for Out-of-Home (OOH) advertising and urban planning. It suggests that a large proportion of potential visual exposure originates from a relatively small number of geographical points, corresponding to buildings at major intersections or prominent corners. This contrasts with planning based solely on average traffic volume because it does not account for driving patterns and visibility considerations (direction and area), which might overlook these high-impact locations or overvalue less visually prominent ones.

Furthermore, the strong adherence of the aggregated visibility counts to a Log-Normal distribution is noteworthy. This statistical characteristic, often found in phenomena involving multiplicative growth or compounding factors, implies that the factors influencing high visibility (e.g., road geometry, traffic speed variations, building prominence, duration of view) likely interact in a way that creates extreme values. This quantitative characterization provides a basis for more sophisticated analysis, such as predictive modeling or differential valuation of potential advertising sites based on their position in the visibility distribution.

The methodology presented, utilizing connected vehicle data, OpenStreetMap features, and efficient BallTree spatial indexing, demonstrates a computationally tractable approach to generating these granular visibility metrics at scale. This represents a significant step beyond traditional static analysis or Opportunity-To-See (OTS) measures, offering objective, data-driven analysis grounded in observed mobility patterns. The resulting quantitative visibility data and hotspot identification

can directly inform strategic decisions regarding the placement of OOH assets like billboards and digital screens, potentially improving campaign reach and effectiveness. Similarly, urban designers and planners can use this information to identify locations requiring high public visibility for signage, street furniture, or public information displays.

Several limitations must be acknowledged. The current visibility model implements a simplified 2D forward-looking circle, which represents the perception area of a vehicle driver. This geometric abstraction does not account for 3D occlusions caused by other vehicles, varying building heights, or roadside vegetation, nor does it incorporate factors central to visual perception like specific viewing angles, the dynamics of driver attention, or the characteristics of the advertisement itself. Future work should focus on enhancing the fidelity of this model, potentially incorporating 3D city models, efficient line-of-sight algorithms with occlusion handling.

Additionally, the connected vehicle data, while providing extensive spatial coverage within the study area (Waterloo, Sydney), represents only a sample of the total traffic volume and diversity. Its representativeness across all vehicle types (private cars, commercial vehicles, public transport) and driver demographics warrants further investigation to understand potential biases in the visibility patterns observed.

#### V. CONCLUSION

This research addressed the need for more accurate, dynamic, and data-driven methods for assessing Out-of-Home advertising visibility in complex urban environments. We developed and demonstrated a scalable computational framework that utilizes large-scale connected vehicle trajectory data (Compass IoT) and open geospatial building data (OpenStreetMap) for the Waterloo area in Sydney. By employing time-based trajectory interpolation, defining a forward-projected viewing area, and utilizing efficient BallTree spatial indexing, our methodology quantifies the cumulative visibility counts for thousands of building vertices based on observed, real-world vehicle movement patterns.

The analysis revealed that building vertex visibility is highly concentrated in specific ‘visual hotspots’ and that the overall distribution of visibility strongly conforms to a Log-Normal model. The primary contribution of this work is the provision of a computationally efficient method for generating granular, objective visibility metrics, offering a significant improvement over traditional static or volume-based assessments. These findings are relevant for optimizing the placement of OOH advertising and street furniture, enhancing urban design, and informing location-based analytics. While acknowledging the limitations of the current visibility model and data scope, this study highlights the substantial potential of combining large-scale mobility data with advanced spatial analysis techniques to better understand and quantify visual exposure patterns within dynamic city environments.

Further research may also explore the temporal dynamics of visibility how patterns change by time of day, day of week, or due to traffic conditions presents another promising avenue for





Fig. 4. Spatial distribution of Building Vertex Visibility, Highlighting Top Quantiles. Different colors represent vertices falling into specific aggregated visibility count percentiles (e.g., Bottom 90%, 90th-95th, 95th-99th, Top 1%).

refining placement strategies. Crucially, validating the derived visibility metrics against empirical data, such as human eye-tracking studies conducted in real or simulated environments, or correlating metrics with real-world advertising campaign effectiveness data, remains an essential step to fully establish the practical predictive power and utility of this quantitative visibility framework. Future work can also be directed towards a bigger scale both in space and time, may focus on analysis of real-time data or calculating change in visibility patterns before, during and after major events.

## VI. ACKNOWLEDGEMENTS

We thank Compass IoT for the data and support provided for this study, especially to Mr David Lillo Trynes. This work has been funded by the UTS Jenny Edwards Fellowship awarded in 2025 to Assoc. Prof. Adriana-Simona Mihaita for conducting research on connected vehicles.

## REFERENCES

- [1] E. Talbot, The great outdoors: An investigation into the value of out-of-home advertising, Masters thesis, Ehrenberg-Bass Institute for Marketing Science, University of South Australia (June 2021).
- [2] K. E. Clow, D. Baack, Integrated Advertising, Promotion, and Marketing Communications, 10th Edition, Pearson, 2023.
- [3] H. Farah, I. Postigo, N. Reddy, Y. Dong, C. Rydergren, N. Raju, J. Olstam, Modeling automated driving in microscopic traffic simulations for traffic performance evaluations: Aspects to consider and state of the practice, *IEEE Transactions on Intelligent Transportation Systems* 24 (6) (2023) 6558–6574. doi:10.1109/TITS.2022.3200176.
- [4] A. S. Matin, Development and evaluation of simulation models for assessing the impacts of connected and automated vehicles (12 2024). doi:10.25916/sut.28087664.v1. URL [https://figshare.swinburne.edu.au/articles/thesis/Development\\_and\\_evaluation\\_of\\_simulation\\_models\\_for\\_assessing\\_the\\_impacts\\_of\\_connected\\_and\\_automated\\_vehicles/28087664](https://figshare.swinburne.edu.au/articles/thesis/Development_and_evaluation_of_simulation_models_for_assessing_the_impacts_of_connected_and_automated_vehicles/28087664)
- [5] N. Huynh, V. L. Cao, R. Wickramasuriya, B. M., P. Perez, J. Barthlemy, An agent based model for the simulation of road traffic and transport demand in a sydney metropolitan area, 2014. doi:10.13140/2.1.4023.2961.
- [6] G. P. Senanayake, M. Kieu, Y. Zou, K. Dirks, Agent-based simulation for pedestrian evacuation: A systematic literature review, *In-*

ternational Journal of Disaster Risk Reduction 111 (2024) 104705. doi:<https://doi.org/10.1016/j.ijdr.2024.104705>.

- [7] K. Maecki, J. Jankowski, M. Szkwardowski, Modelling the impact of transit media on information spreading in an urban space using cellular automata, *Symmetry* 11 (2019) 428. doi:10.3390/sym11030428.
- [8] Handbook of mobility data mining, volume 3: Mobility data-driven applications, in: H. Zhang (Ed.), *Handbook of Mobility Data Mining*, Elsevier, 2023. doi:<https://doi.org/10.1016/B978-0-323-95892-9.01001-9>.
- [9] P. Chao, A study on map-matching and map inference problems, Phd thesis, School of Information Technology and Electrical Engineering (Aug. 2020). doi:10.14264/uql.2020.1009. URL <https://doi.org/10.14264/uql.2020.1009>
- [10] P. Rathore, D. Kumar, S. Rajasegarar, M. Palaniswami, J. C. Bezdek, A scalable framework for trajectory prediction, *IEEE Transactions on Intelligent Transportation Systems* 20 (10) (2019) 3860–3874. doi:10.1109/TITS.2019.2899179.
- [11] A. Y. Xue, J. Qi, X. Xie, R. Zhang, J. Huang, Y. Li, Solving the data sparsity problem in destination prediction, *The VLDB Journal* 24 (2) (2015) 219–243. doi:10.1007/s00778-014-0369-7. URL <https://doi.org/10.1007/s00778-014-0369-7>
- [12] H. Farooqi, M. Mesbah, J. Kim, A. Khodaii, Targeted Advertising in the Public Transit Network Using Smart Card Data, *Networks and Spatial Economics* 22 (1) (2022) 97–124. doi:10.1007/s11067-022-09558-9. URL <https://doi.org/10.1007/s11067-022-09558-9>
- [13] S. Fong, K. Cho, W. Ip, E. Liu, Identifying optimal spatial groups for maximum coverage in ubiquitous sensor network by using clustering algorithms, *International Journal of Distributed Sensor Networks* 2013 (07 2013). doi:10.1155/2013/763027.
- [14] S. Liu, Y. Zheng, X. Liu, W. Ke, V. W. Zheng, H. Qu, SmartAdP: Visual analytics of large-scale taxi trajectories for selecting billboard locations, in: 2016 IEEE Pacific Visualization Symposium (PacificVis), 2016, pp. 48–55. doi:10.1109/PACIFICVIS.2016.7465251.
- [15] Y. Xiao, J. Xu, M. Chraibi, J. Zhang, C. Gou, A generalized trajectories-based evaluation approach for pedestrian evacuation models, *Safety science* 147 (2022) 105574.
- [16] C. Kerouanton, L. Jolivet, C. Perrin-Malterre, A. Loison, Eye-catching or breath-catching: Role and landscape attributes of pauses differs among hikers profile when rambling in a french mountainous area, *Journal of Outdoor Recreation and Tourism* 46 (2024) 100734. doi:<https://doi.org/10.1016/j.jort.2024.100734>. URL <https://www.sciencedirect.com/science/article/pii/S2213078024000021>
- [17] C. Gschwend, Relating movement to geographic context: effects of preprocessing, relation methods and scale, Ph.D. thesis, University of Zurich (2015).